Foveal drusen increase fixation instability: fixational eye movements as biomarkers for pre-symptomatic AMD.

Abstract

Purpose: To link changes of fixational eye movements (FEM) in controls and patients with foveal drusen using adaptive optics retinal imaging to find biomarkers for pre-symptomatic AMD.

Design: A nationwide population-based cohort study.

Participants: 7 young controls, 4 older controls and 16 pre-symptomatic dry-AMD patients with foveal drusen.

Methods: On one side monocular retinal tracking was performed on a research-grade adaptive optics flood illumination ophthalmoscope. The system allows for sub-arcminute resolution, high-speed, and distortion-free imaging of the foveal area. We extracted then compared microsaccade and drift characteristics across individuals and groups. On the other side, screening of foveal drusen was performed on older subjects using gaze-dependent protocol on a clinical-grade AO-FIO. We then annotated drusen from resulting images to determine their location and size.

Main outcome measures: The difference in microsaccade amplitude, drift diffusion coefficient and fixation stability with ISOline Area (ISOA) between groups. For the drusen group, the relationship between these variables and retinal structure characteristics: drusen size and eccentricity in the fovea.

Results: FEM were measured with high precision (RMS-S2S=0.001°) and small drusen (median=60µm) were detected with high contrast imaging. Microsaccade amplitude, drift diffusion coefficient and ISOA were significantly larger for patients with drusen compared with controls. Among the drusen participants, microsaccade amplitude was correlated to drusen eccentricity from the center of the fovea.

Conclusions: A novel high-speed high-precision retinal tracking technique allowed for the characterization of FEM at the microscopic level. Foveal drusen altered fixation stability, resulting in compensatory FEM changes. Eye movement analysis with flood imaging provides robust description of both functional and structural signs of early age-related changes.

Introduction

Age-related Macular Degeneration (AMD) is the main cause of vision loss in developed countries, affecting 180M people in 2020 with an expected prevalence of 288M by 2040[1]. AMD can be either exudative (wet-AMD) or atrophic (dry-AMD)[2]. Wet-AMD is caused by irregular blood vessel growth (i.e., neovascularization) at the macular level, and it affects approximately 10-20% of AMD patients[3]. Wet-AMD can be treated using anti-VEGF before it becomes a threat to the patient's vision. On the other hand dry-AMD starts with the accumulation of extracellular deposits, called drusen, in-between the Bruch's membrane and the RPE, and it accounts for about 80 to 90% of the cases[2]. Dry-AMD has become a major public health concern as no effective treatment currently exists and little is known about the drusen development in asymptomatic stages. The remaining action someone with high probabilities of developing dry-AMD can do is risk reduction management such as health style changes and food supplements. These have been shown to be closely correlated with disease progression[4]. However, patients are mostly unaware of having AMD[5] and usually get diagnosed when clinical signs appear, often too late for these preventive measures[6], therefore showing the importance of a presymptomatic detection of dry-AMD. Early detection would also allow testing of clinical therapies being developed to slow down drusen accumulation and geographic atrophies growth[6].

The development of AMD has already been associated with decreased visual acuity, reduced visual field, slower reading speed, lower contrast sensitivity and an overall deterioration of functional vision useful for daily activities[7–9]. More specifically, fixation stability has been studied in early to late AMD, and it has been shown to worsen with the stage of the progression[10]. However, it is only in 2014 that fixation stability in macular degeneration was studied through the analysis of fixational eye movements[11]. During periods of visual fixation, the gaze does not remain completely still. Unaware of it, people still produce micro eye motion that has been named fixational eye movements (FEM). Slow ocular drifts move the eye

according to a random brownian walk[12] and are interrupted by fast and short microsaccades that occur 1-2 times per second with amplitudes below 1° [13]. Ocular tremor are high frequency sub-arcminute oscillations taking place during the drift[14]. Kumar showed that microsaccade amplitude is significantly larger in patients with lesions due to macular degeneration, therefore increasing fixation instability[11]. Using the same set of participants, Ağaoğlu focused on ocular drift and observed less spectral whitening of natural scenes in patients with geographic atrophies[15]. While these two papers show clear signs of changes in fixational eye movements on patients with advanced forms of AMD, they remain exploratory and the patients already are at an advanced stage of AMD. Authors did not seek a biomarker for early to presymptomatic cases, nor characterize the links between the characteristics of retinal structure changes and FEM.

While to the best of our knowledge alterations of oculomotor control with small changes of retinal structure have never been studied, the application of eye movements to identify biomarkers of any kind of disease is not new. Eye movements can reveal information about neurological disorders or retinal integrity and could provide non-invasive biomarkers[16]. However, FEM are trickier to study because of both the high precision and high speed eye-tracker requirement. Challenges arise especially when it comes to translating those high precision eye tracking methods from labs to clinics and hospitals. In research, FEM have mostly been explored in neurological disorders such as amblyopia[17], schizophrenia[18], Parkinson's disease[19] and few more[20]. Nonetheless, there have been recent attempts to reveal new biomarkers from FEM that have relied on microsaccadic intrusion occurrences to predict multiple sclerosis and follow its development[21] or fixation abnormalities in amblyopia to assess treatment efficiency[22]. In our case, an important challenge that came with the study of FEM changes with respect to small asymptomatic alterations of retinal structure such as drusen is the use of novel high resolution imaging methods to efficiently characterize those pathological retinas. We believe the lack of studies that explore that path might come from the low number

of protocols to visualize drusen as well as the difficulty to gather a large cohort to find participants before clinical signs appear.

In this study, we studied FEM in relation with healthy aging and dry-AMD at a presymptomatic stage. Participants in the latter group have developed foveal drusen but no scotoma or atrophy yet. Importantly, this condition might not necessarily degenerate into dry-AMD. This definition rather reflects a higher risk for dry-AMD onset with respect to normal eye senescence. The first objective was to link changes in FEM with subtle retinal structure variations induced by the drusen. This required to both estimate FEM with high resolution and to precisely image and characterize drusen position and size. To the best of our knowledge this level of precision in drusen characterization combined with eye movement exploration has never been studied and could help better understand how oculomotor behavior reacts to the appearance and development of drusen. Then, if patients with foveal drusen are confirmed with higher fixation instability at this stage, we aimed at identifying which FEM components modification carry the potential to become biomarkers for the presence of drusen in the foveal region.

Methods

Participants

A cohort of 39 participants were recruited for the study as part of one of three groups: young controls, older controls, and the drusen group. They were all recruited from the SilverSight cohort, fully screened and ascertained not to suffer from any age-related sensory, cognitive or motor pathology. Drusen were first revealed by OCT imaging by orthoptists and ophthalmologists. Before the beginning of the experiment, each participant from the older controls and the drusen group were imaged using a commercial clinical-grade *Adaptive Optics Flood-Illumination Ophthalmoscope* (AO-FIO) (rtx1, Imaging Eyes) and following the gaze-dependent protocol described by Rossi et al.[23]. This allowed for a more precise visualization of the drusen in the foveal region than the standard OCT detection (see paragraph below). Therefore, many participants first recruited as older controls were found to have drusen in the foveal region and were switched groups. Three participants had too blurry images for the gaze-dependent protocol when using the rtx1. Three participants had to stop the experiment due to poor signal-to-noise ratio during the high-speed recordings of the fixation task. Two participants' data had to be discarded because they were not fixating at the right target. Three participants were not included in the study because of excessive tiredness due to the length of the experiment and discomfort on the bench.

Overall, 7 young controls([2 females], age=31±7 yo), 4 older controls ([1 female], age=72±2 yo) and 16 drusen patients ([10 females], age=74±4 yo) were kept for the study and their visual characteristics are given in **Table 1**.

Ethics Committee approval (CPP) was obtained. Our clinical, experiment and data management procedures adhered to the tenets of the Declaration of Helsinki. All participants were part of the SilverSight cohort of the Vision Institute (Paris, France) and a signed consent was obtained to participate in the study (ID_RCB 2015-A01094-45, n. CPP: 16122 MSB) as

well as for the inclusion to the Multimodal Ophthalmologic Imaging protocol (IMA-MODE, ID_RCB 2019-A00942-55 CPP: Sud Est III 2019-021-B) of the Quinze-Vingts National Ophthalmology Hospital.

Table 1: Demographic data and visual characteristics of participants enrolled in the study.

Tag	Age (yo)	Tested eye	Visual acuity	Number of drusen	Mean drusen area ± std (arcmin²)	Mean drusen eccentricity ± std (arcmin)
ALG	78	OD	1	7	153 ± 60	28 ± 23
ATA	74	OD	1	2	96 ± 26	45 ± 14
BEH	70	OS	1	6	162 ± 36	56 ± 32
BEY	81	OD	1.2	8	112 ± 58	69 ± 42
ATM	75	OD	1.2	20	167 ± 35	68 ± 34
BLJ	76	OD	1.2	28	172 ± 68	92 ± 34
DEB	73	OD	0.8	4	120 ± 33	62 ± 22
DEC	80	OD	1	5	68 ± 16	30 ± 25
LED	79	OD	1.2	7	72 ± 13	27 ± 22
LES	76	OS	1	9	119 ± 66	45 ± 27
MAC	80	OD	0.7	6	116 ± 45	68 ± 19
NAM	74	OS	0.8	14	53 ± 14	76 ± 25
OLD	84	OS	1	13	161 ± 44	63 ± 25
PEF	80	OD	1.2	32	307 ± 134	49 ± 31
PEN	83	OS	1	12	160 ± 46	42 ± 26
ROM	84	OS	1.2	7	129 ± 29	37 ± 29
Total (Drusen group, n=16)	**78 ± 4**	**/**	**1 ± 0.2**	**11 ± 8**	**133 ± 59**	**53 ± 27**
Older adults (n=4)	**72 ± 2**	**/**	**>1**	**/**	**/**	**/**
Young adults (n=7)	**31 ± 7**	**/**	**>1**	**/**	**/**	**/**

Gaze-dependent imaging and drusen visualization

All subjects underwent a SD-OCT (Spectralis OCT, Heidelberg Engineering, Germany) scan in order to reveal potential foveal drusen. Gaze-dependent retinal fundus imaging of their central retina was performed using a rtx1 AO-FIO following the method and protocol described by Rossi et al.[23]. Compared to direct single retinal flood imaging, gaze dependent imaging computes the local maxima of contrast across a stack of 5 images whose gaze direction has been sequentially shifted. A 4° fovea-centered image of the retina, focused on the photoreceptors, and four ±1° horizontally and vertically displaced images (with respect to the center image). After image registration, the maximum of the standard deviation for each x, y pixel of the 5-image stack is computed to make gaze-varying structure visible. The resulting contrast image provides a vivid imaging of drusen and their delineation, hence more precise information about their size and position compared to existing methods. Hence gaze-dependent imaging allows for the visualization of smaller drusen in the fovea than standard methods. All the image filtering, registration and processing were made using a MATLAB custom software.

In a final step, drusen were manually annotated as ellipses using a MATLAB custom built interface. Two experts in medical images performed this procedure after training and validation by two ophthalmologists.

Experimental protocol

Participants had their dominant eye dilated with a drop of 1% tropicamide (*Mydriaticum*, tropicamide 0.5%). Then, in a dark room with minimal stray light, they placed their head on a chinrest where video recordings of their fovea were made using an *Adaptive Optics Flood-Illumination Ophthalmoscope* (AO-FIO) (see below). The task consisted in fixating a circle (outer diameter: 17 arcmin (0.28°), inner diameter: 11 arcmin (0.18°)) for 30 seconds, across 5 trials. The instructions were *"Please, fixate the circle for 30 seconds. Do not speak and try not moving your head. Do not hesitate to blink if you need to.",* and a vocal indication about

time progression was provided after 15 seconds. The stimulus projection with the DMD was controlled using a custom-made Python code and the ALP4Lib python library wrapper. The adaptive optics loop was controlled with a LabVIEW program and image acquisition was monitored via Holovibes software.

Retina imaging setup

Foveal video recordings focused on the photoreceptor layer were made possible by an *Adaptive Optics Flood-Illumination Ophthalmoscope* (Paris AO-FIO) developed by ONERA[24] and located at the Quinze-Vingts National Ophthalmology Hospital in Paris, France. Concurrently with high-resolution structural imaging of the retina, the Paris AO-FIO allows for the projection of NIR illumination patterns (i.e., stimuli) onto the retina via a deformable Digital Micromirror Device (DMD)[25] (Krafft 2021a) as well as for partial-field illumination[26]. The system consists of two optical channels: the Wavefront correction channel, and the illumination and imaging channel, combined with the stimulation channel. A fibered SuperLuminescent Diode (Exalos, Switzerland) with nominal center wavelength of 750 nm measures optical aberrations, and an 850nm LED source (Thorlabs, USA) coupled with a liquid fiber homogeneously illuminates the retina over a 4° diameter field of view (**Fig. 1a**). The adaptive optics compensated for the spherical, cylindrical and some higher order aberrations of the eye's optics before the stimulus reached the retina. The backscattered light from the eye was reflected back on the deformable mirror before reaching the imaging camera.

Retina motion tracking

Prior to the beginning of the task, participants were required to fixate a central cross for 5 seconds. A full field sequence of images covering a 4° diameter field of subjects' retina was recorded at 100 Hz (2048 x 2048 pixel frames) during the 5 s period. The recorded full field retinal images were first stabilized and then averaged into a unique full field reference frame of the center of the retina (**Fig. 1a**). Then, during the task, only a sub-band (2° x 0.5°, 1400 x

256 pixel, with the black circle target at the center) was recorded at 800 Hz to be used for retina motion tracking (**Fig. 1b**).

Retinal motion was tracked using a phase-correlation registration method[27] after bandpass filtering the image sequences. The algorithm consisted in finding the position that best fitted each frame of the high speed video onto the reference image. The best fit was considered as the peak value coordinates of the correlation map computed in the Fourier domain.

Even if the maximum sampling frequency of the camera was only limited by vertical pixel resolution, we found that 1400-pixel horizontally offered a good tradeoff between field coverage and video bandwidth. The resulting 0.684 MB/frame (16 bits) led to a very large 547 MB/s video bandwidth that could only be recorded with solid state hard drives and ad-hoc recording software (Holovibes). Videos were recorded on a separate computer than the one used for stimulus presentation.

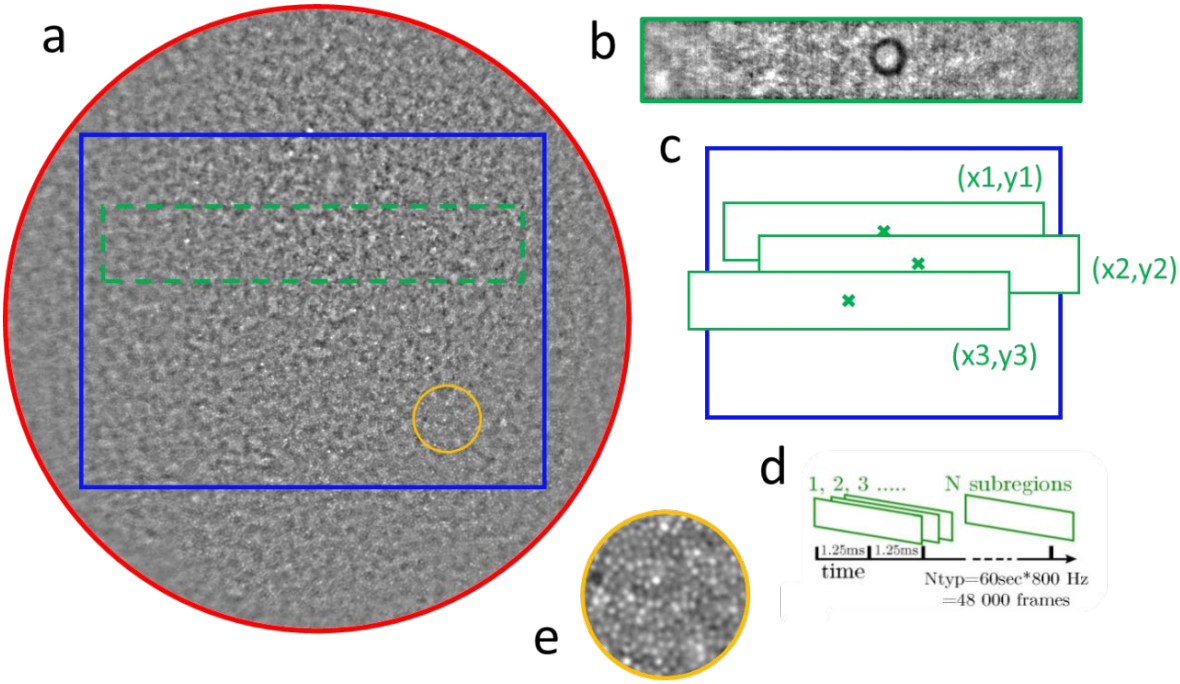

Figure 1. Principle of the AOFIO retinal tracking. **(a)** The 4° full field obtained after a 5-sec recording at 100 Hz after registration (red). A rectangular sub-part (blue) is enough to track and monitor eye movements on tasks requiring central fixation (typ. <2°). The 2 x 0.5° subregion (green) is tracked at very high speed . **(b)** An actual frame recorded at 800 Hz on 16 bits. **(c)** The displacement is obtained by a search (phase-correlation) over the rectangular full-field. **(d)** An ad hoc eye position extraction software processes large sequences of up to 5 Mbits/frames. e. A 3x zoom on an area 1° away from the fovea.

Detection of retina motion related events

Processing of the raw pixel displacement of each frame relative to the reference images to ocular movement in arcminutes with annotated events was made with a MATLAB (Mathworks, USA) custom program. Microsaccades were detected using an acceleration threshold inspired by Engbert[28]. An acceleration, rather than velocity, threshold (factor N=3 standard deviation of the median) was used in order to differentiate fast ocular drift epochs from small and slower microsaccades which can have similar velocities but distinct accelerations. The acceleration was computed for the 30 s fixation, and smoothed over 70 ms windows. This adaptive algorithm allowed for thresholds that fitted both participants with small microsaccades (as small as 1 arcminute) and stable ocular drift, and participants with larger microsaccades and drift amplitudes. However, to ensure that microsaccades were all entirely detected and that some parts of ocular drift were not mislabeled as microsaccades, all traces were manually verified after the automatic annotation. Blinks were detected automatically as sudden drops in mean frame pixel intensity, which corresponded to the closed eye reflecting less light back to the camera. Rejected data were epochs of ocular coordinates marked by the user as false data due to failures in the imaging or the tracking (to the exclusion of blinks). They accounted for 0-3% of the fixation data for each participant. Everything in-between two events – microsaccades, blinks or rejected data– was automatically marked as drift. An example of a 3-second fixation is shown in **Fig. 2** with eye motion coordinates and annotated events.

Figure 2. Eye traces of a healthy young subject (top) vs a subject with drusen (bottom) with the corresponding movement in the visual field. The eye traces are shown for 3 seconds. Microsaccades are annotated in pink and drift in light blue. Eye position is shown in degrees. The green line is the ISOA 86%

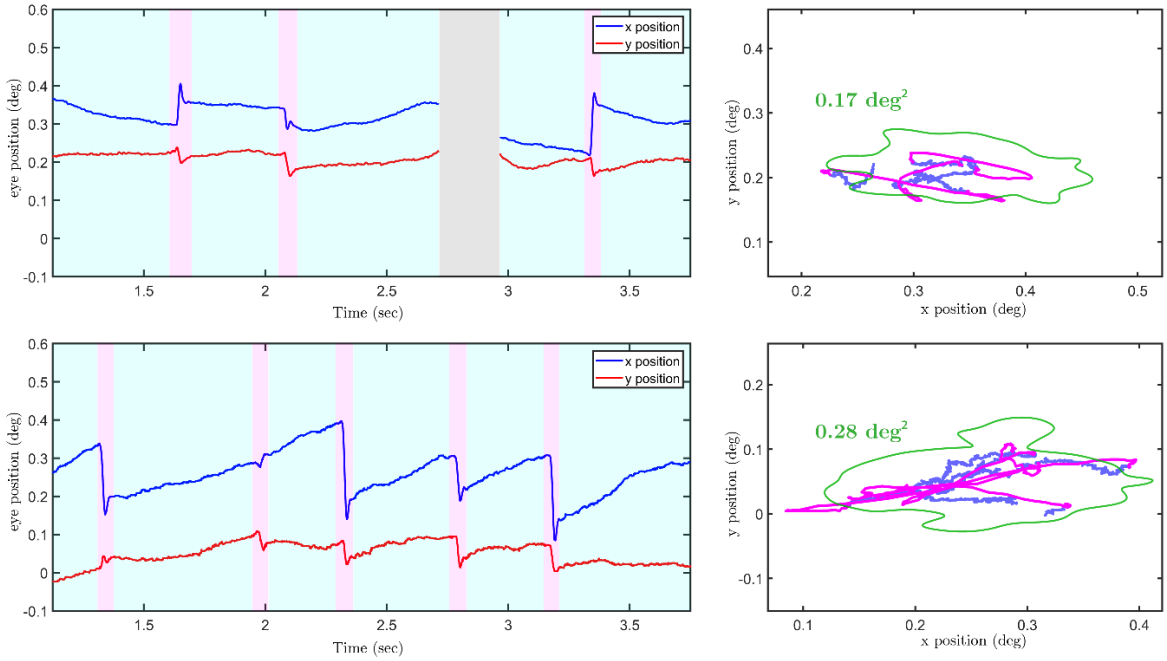

Estimation of fixation stability

The Bivariate Contour Ellipse Area (BCEA) and more recently the ISOline Area (ISOA) metrics have been used to clinically measure fixation stability of patients with central vision loss, including AMD[29]. Because ISOA is more robust than BCEA as it can delineate non-ellipsoidal fixation patterns[30] and can be used to detect possible multiple retinal fixation loci, PRLs, such as in AMD patients. The choice of the bandwidth and the extent (i.e., number of standard deviations) to compute the ISOA is relatively arbitrary and open to criticism[30–32]. The choice of a 1° window for Kernel Density Estimation (KDE) has been shown to be robust and appropriate with respect to a classical definition of the 1° foveola[31,32] (Martinez-Conde, 2006; Otero-Millan *et al,* 2008). Concerning the ISOA contour extent, we used both the standard 68% ISOA (i.e., encompassing 68% of the data points) and the 86% ISOA (i.e., computed over 2 standard deviations in the 2D space defined from the center of the fixation distribution; Wang et al. 2015). The rationale was that the 86% ISOA contour would provide complementary insights

on the global fixation pattern that might better differentiate healthy controls from participants with foveal drusen.

Drift diffusion coefficient and amplitude spectrum computation

In the framework of Brownian motion[12,33], the eye movement during the drift epochs can be modeled by a random walk, and the general motion can be measured by the diffusion coefficient *D*. This was computed by least square best fit to the measurements of the empirical standard deviation of the eye displacement as a function of time[34]The motion amplitude spectra of the ocular drift segments were then analyzed by using a multitaper spectral analysis. This analysis was carried separately on the horizontal and vertical components of eye motion[35,36], on overlapping segments of 1 s. The time half-bandwidth product was fixed at 2.5, and the last taper was dropped to maximize spectral concentration ratios in the Slepian sequences.

Results

Robustness and precision of retinal imaging and tracking method

Robustness of the PARIS AO-FIO imaging system can be visually assessed thanks to the full field images of the center fovea. Regardless of lens opacity affecting over half of the older patients, individual photoreceptors were still distinguished (**Fig. 1e**).

Root mean square sample to sample (RMS-S2S) deviation was calculated as a way to measure the precision of the retina tracking method. A given RMS-S2S of an eye-tracker would mean the average movement due to noise between successive data is its squared value[37,38]. Since the ocular traces used in this tracking method were not filtered, which has a strong effect of RMS-S2S and skews the results[39], it appeared to be the right metric to measure tracking precision. The average RMS-S2S across all participants was 0.001°, and 0.0001° on a non-moving model eye (OEMI-7 Ocular Imaging Eye Model). Low standard deviation (σ=0.0005°) also demonstrated great robustness for the method.

The power spectrum of the non-moving model eye is one to two orders of magnitude below human participants, displaying negligible noise coming from factors such as vibrations or mathematical failures of the tracking algorithm. For all groups, power spectra were not very noisy, even in higher frequencies (above 100Hz), often more challenging to visualize.

The high precision of the retinal tracking method allowed microsaccades as small as one or two arcminutes to be easily visualized and detected (**Fig. 2**).

Detection and characterization of foveal drusen

Foveal drusen information was extracted from gaze-dependent images by manually drawing ellipses around them as displayed in **Fig. 3**. The number of drusen, the eccentricity from the center of the drusen to the center of the fovea, the areas, the diameters of the ellipses (average of small and large diameter) and total area covered by all drusen were computed. Individual

information about drusen are given in **Table 1** as well as average number, size and eccentricity. Overall distribution of drusen diameters is given in **Fig. 3** with a median value of 60 µm. 11 participants recruited as control older adults with no drusen detected on OCT images were switched to the drusen group.

Participants from the drusen group were subsequently split into two subgroups based on the eccentricity of their drusen. By taking into account the approximate size of the foveola (0.4-0.6° [40]), the stimulus diameter (0.28°), and the median foveal drusen diameter in this study (0.2°), the two subgroups were taken as follow: those participants with drusen mainly in their foveola (mean drusen eccentricity less than 1° away from the center of the fovea); and those participants with drusen mainly outside their foveola.

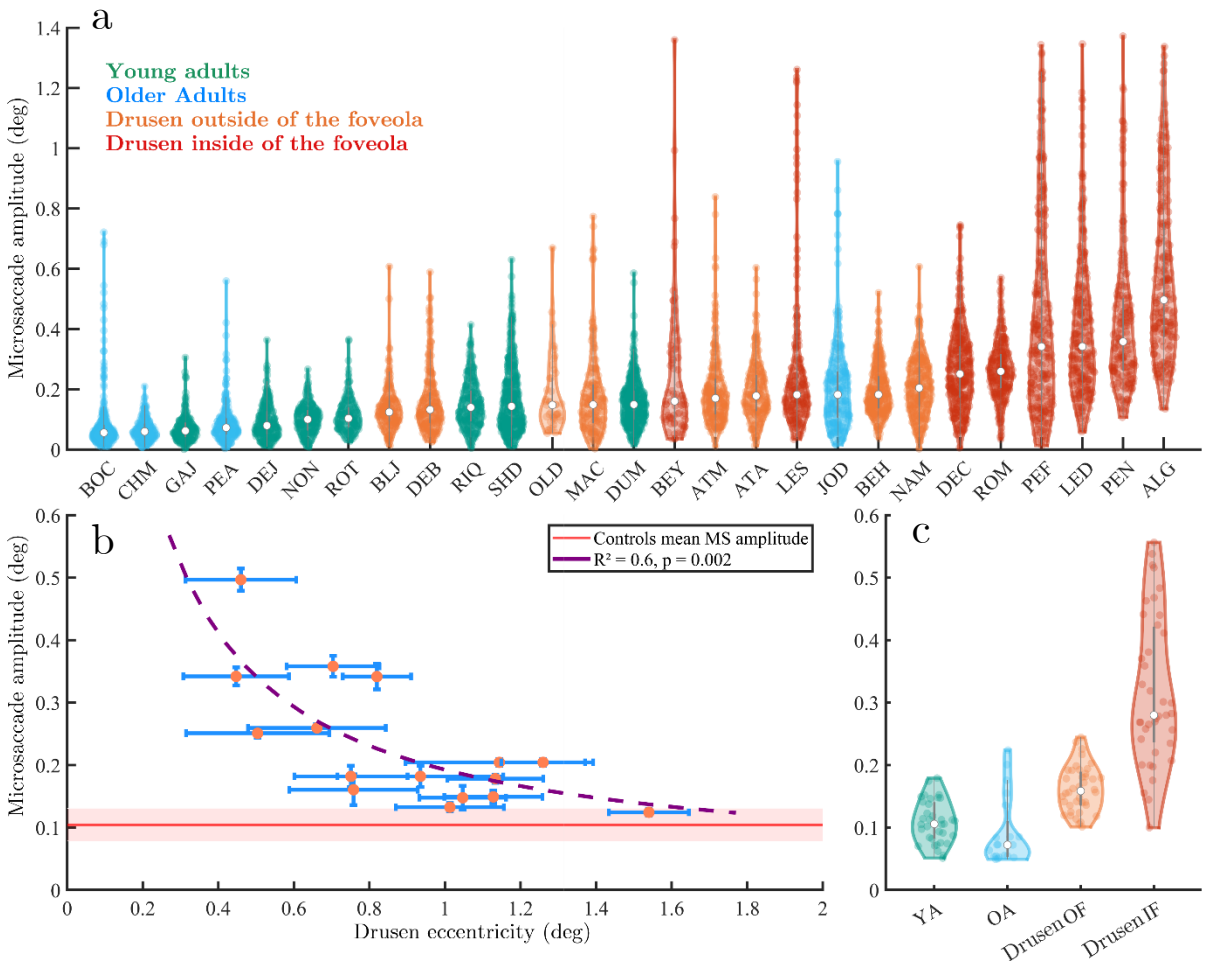

Figure 4. Microsaccade characteristics across individuals and groups. **(a)** Individual microsaccade amplitudes distribution across all participants, color-coded by group and sorted with respect to the mean microsaccade amplitudes. Each dot is one microsaccade during the fixation task. **(b)** Microsaccade mean amplitude with respect to drusen eccentricity from the center of the fovea. Standard errors are shown in blue bars. **(c)** Microsaccade amplitudes across all four groups. Each dot is one trial.

Individual distributions of microsaccade amplitudes can be found in **Fig. 4**, sorted from lowest mean amplitude to highest and color-coded according to their groups. Healthy participants were overall shifted to the lowest amplitudes and pathological participants to the highest ones, but mean amplitudes seemed distributed on a relatively continuous function with no clear separation. When scatter plotting mean microsaccade amplitude with ISOA (**Fig. 7**), participants with drusen inside their foveola are clustered around higher values.

T-tests and linear mixed effect statistical model analysis revealed significant differences between the microsaccade amplitudes of the drusen-inside-the-foveola group and the three other groups ($|t|>5$, $p<10^{-5}$). The drusen-outside-the-foveola group had overall larger microsaccades than young and older adults although the difference was marginally significant (respectively $|t|=1.7$, $p=0.09$ and $|t|=1.6$, $p=0.06$). There was weak difference between young and older adults ($|t|=0.4$, $p=0.66$).

As a first step to finding a correlation between drusen and fixation, a simple linear correlation map was computed using different drusen and fixational eye movements characteristics. The most significant correlations were found for mean microsaccade amplitudes compared to mean drusen eccentricities ($r<0$, $r^2=0.52$, $p=0.001$). The negative correlation reveals that microsaccades get larger the closer drusen are to the center of the fovea. However, as made in evidence in **Fig. 6**, the best correlation was not using a linear regression but by fitting a rational function to the scatter plot ($r^2=0.6$, $p=0.002$). The closer drusen are to the center of the fovea, the larger microsaccades are, but the further away drusen are, the more subjects tend to produce microsaccades similar to controls.

Finally we hypothesize that more than drusen eccentricities, or their local density, it's their density related to their eccentricity that might best reflect their influence on fixation stability. The rapid drop-off of both cone density and acuity in the fovea suggest that both drusen size and eccentricity can have tremendous effect on foveal vision. We then reported drusen areas divided by their eccentricities. The mean drusen density was also even further correlated to

microsaccade amplitude (p=0.0002, r^2=0.66) but with higher standard deviations for each participant.

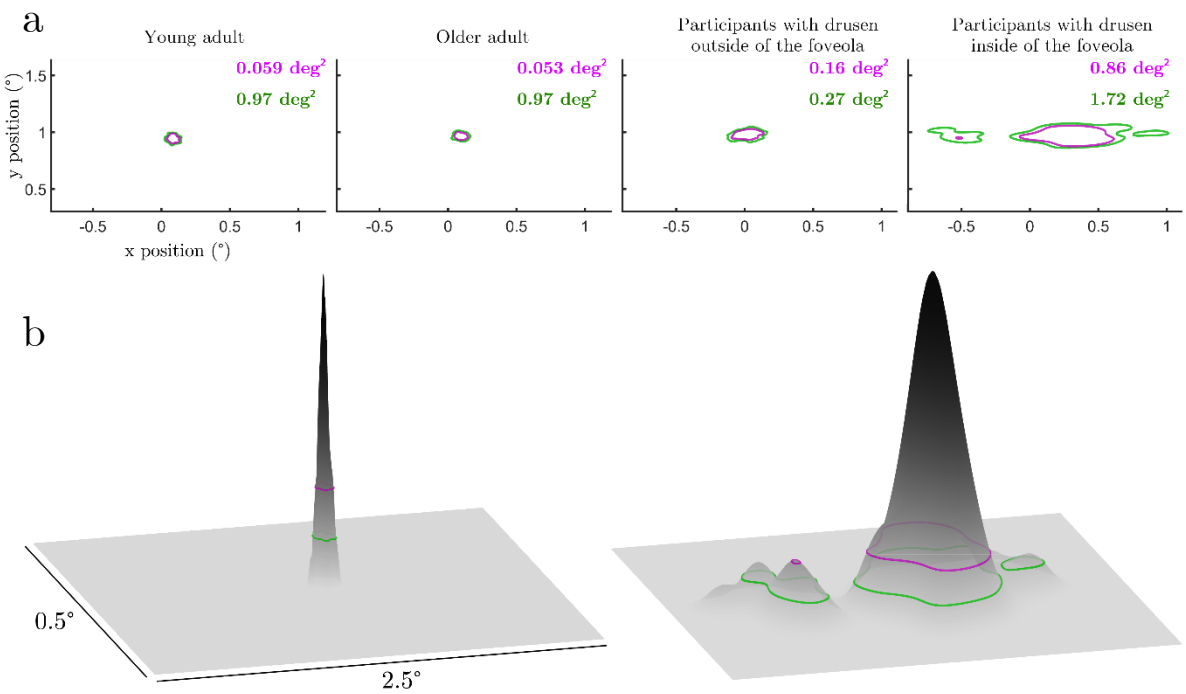

Figure 5. Impact of drusen on fixation stability. (a) The top row shows sample data respectively from a young adult, an older adult, a participant with foveal drusen and a participant with foveolar drusen. **(b)** Probability density of the young adult participant of (a) on the left and the foveolar participant of (a) on the right. ISOA contours encompassing 68% (purple) and 86% (green) of the eye position data.

Impact on fixation stability

The same tendency as with microsaccade amplitude was found when comparing 86% ISOA values, which is consistent with microsaccade amplitude and ISOA being highly correlated (**Fig. 4a,** r^2=0.85). All t-values and p-values can be found in **Table 2**. The isoline contours 68% and 86% are shown in **Fig. 5**. The ISOA approach offered an interesting topology of the shape of the fixation instability. This shape appeared specific to each participant, especially for those with higher instabilities. However, the participants with the highest ISOA -from the drusen groups- had contours with very different patterns and islands, and not simply a uniform larger area shape. While some fixations expanded more on the horizontal axis, a few participants

had their fixation area grow on the vertical axis, and a couple of them started creating multiple loci of fixation. Overall, these specificities were more visible using contours encompassing 86% of the fixated locations than 68%. In this study, there were no significant differences in microsaccade rate between groups that could explain the differences observed in fixation stability and almost every participant had a normal microsaccade rate of 1-2 Hz.

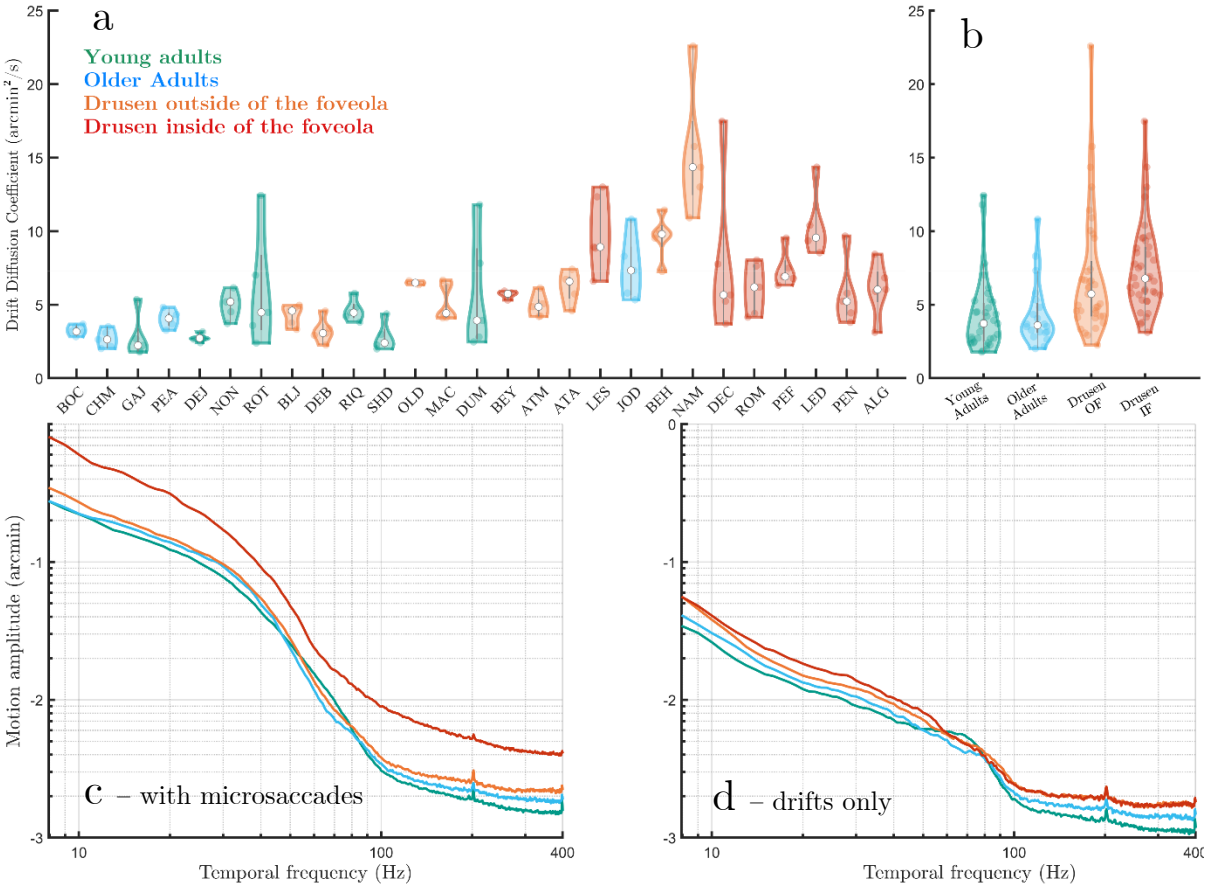

Figure 6. Drift dynamics and motion spectra across groups – horizontal motion. **(a)** Drift diffusion coefficient distribution across all participants, sorted with respect to mean microsaccade amplitudes. Each dot is one trial. **(b)** Significant differences in drift coefficient were found between the healthy groups and the group with foveolar drusen, as for microsaccade amplitude. Drift motion contribute to the impeded fixation stability (**Fig. 5a** vs **5b**) except for the foveolar drusen group. **(c)** Motion spectrum across the four groups. An increase in drift dynamic across most frequencies is visible with age, and even further with the presence of foveal or foveolar drusen. This progressive increase is particularly visible in the Mid-frequency (10-40 Hz, top left inset) and very-high frequency range (100-400 Hz, top-right inset). **(d)** Motion spectrum of drifts only across the four groups.

Impact on ocular drift

Similarly, t-tests and linear mixed effect statistical model analysis revealed significant although weaker differences in the drift diffusion coefficient between the group with foveolar drusen and both the young and older group (**Table 2**). The group with drusen outside their foveola had only significant difference in drift diffusion coefficient with the young group. Individual diffusion coefficient revealed larger inter- and intra-variability (**Fig 6a**) as well as within- and between-groups (**Fig 6**) when compared to mean microsaccade amplitude (**Fig 4a**).

Impact on motion spectrum

An analysis of the motion spectrum revealed a progressive increase in the motion components of the drift with age and drusen centrality (**Fig 6c**), in the middle frequency range (10-40 Hz, see **Fig 6c left inset**). The high frequency motion within the 2 drusen groups drusen appears of similar amplitude however (**Fig 6C right inset**). When accounting for the motion brought by microsaccades, the foveolar drusen group stands out across all motion frequencies indicating greater impediment for later-stage neural processing[34].

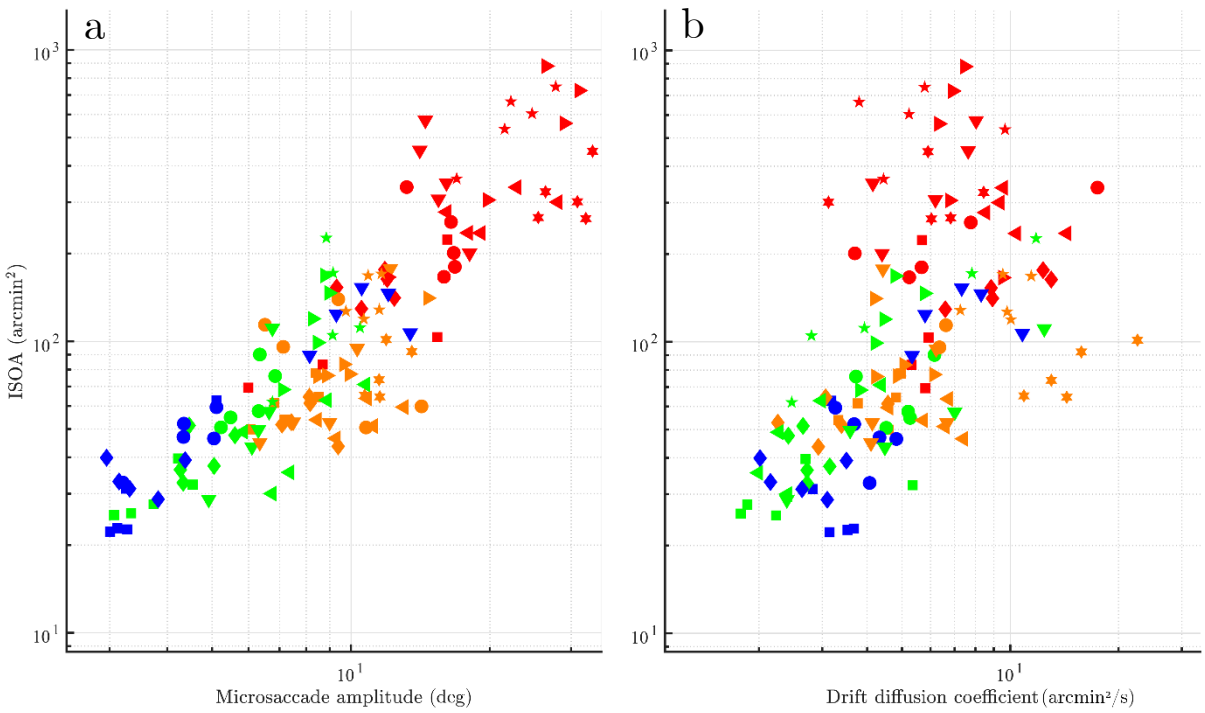

Figure 7. Contribution of microsaccade amplitude and drift coefficient to fixation stability. (a) Microsaccade amplitude vs. 86% ISOA. **(b)** Drift coefficient vs. ISOA on the right. One symbol represents one trial of a participant from its colored group.

Discussion

In this study, we aimed at understanding the consequences of foveal drusen on fixational eye movements in older adults. We used a novel method to track FEM by imaging the foveal region of the retina with high speed, high resolution and no distortion thanks to an AO-FIO that could also project stimuli for psychophysical testing. We consequently tracked the eye movements with one of the highest precision we can find in literature and no motion artifacts, with an instrument robust to lens opacities. In order to understand and further quantify the role of structural markers on functional vision, we used a recently developed enface drusen identification method[23]. We found that patients with drusen exhibited significantly larger microsaccades and fixation instability while maintaining similar microsaccade rates compared to healthy control subjects. Among that group, the drusen eccentricity to the center of the fovea was the main source of the larger microsaccade amplitudes and ISOAs. Indeed, the closer the drusen were, the more unstable the fixation was. The further away the drusen were, the more the participants tended to behave like control subjects, with minimal to no changes in fixation stability.

There appears to be an inflexion point from which drusen eccentricity had less influence on fixation characteristics. We observed that microsaccade amplitude starts increasing much faster when drusen are closer than around 0.8° to 1°. Patients with drusen further than that only exhibited a minimal increase compared to controls with less variability among this group. Considering the size of the drusen and the fixation target, we hypothesized that the limit at which drusen start to disturb fixation is at the foveola, the 350 µm foveal pit as defined by Kolb[40]. The function of microsaccades is still a matter of debate but many researchers agree that they serve different purposes within the foveola, and take its size as a reference to define microsaccades[13,41]. As discussed in Poletti's review on attention and eye movements at the foveal scale[41], any stimuli in the foveola can be attention-grabbing and whether it is voluntary or not, it is possible to have microsaccade directed towards different stimuli as close as 20

arcminutes from each other. Drusen probably does not constitute specific inputs to visual processing but they might change retinal processing in specific retinal locations. Drusen might locally influence perception and therefore affect fixation, especially when located in the foveola. If so, a fixation test could be suitable to discriminate healthy participants to ones having retinal anomalies in the foveola, such as drusen, and it would focus on microsaccade amplitude and ISOA.

The impact of drusen density and centrality on the diffusion coefficient of the drift -a displacement estimator reflecting the randomness and stability of the visual processing- exist at the group level but were individually less apparent. While there was marked difference between the control groups and the foveolar drusen group, and marginal difference with the foveal drusen group, the drift diffusion coefficients of individuals with foveolar drusen did not drive their poorer fixation stability. Drift can be modulated by visual acuity, fatigue or comfort so it is possible that it revealed indeed more than structural defects. The motion spectrum of the drift epoch appears however impacted by the presence of drusen and their centrality, especially in the middle frequency range. But the motion spectrum of the whole eye movements including microsaccades was offset across all the frequency range; first by age, then by the presence of foveal drusen and finally by the presence of foveolar drusen.

Another interesting observation made in this study concerns the definition of *healthy older adults*. Many of them were recruited as healthy controls because no visible drusen were found on the fovea using SD-OCT imaging analyzed by doctors. However, using gaze-dependent imaging, a lot of them were found with drusen in their fovea. Dry-AMD always starts with the development of small drusen but the sole presence of small hard drusen does not imply that the patient will evolve into later stages of AMD[42]. Our observation aligns with findings suggesting that drusen appearing under the retina are highly prevalent and part of normal aging[43,44]. However, no recent studies with more advanced imaging techniques have been conducted to confirm those hypotheses. That could also clarify why some studies reported differences in fixation stability between young and older adults[45–47], while others -including

ours- did not[48–50]. If exhibiting foveal drusen is a common trait within older participants that affect fixation stability, studies would not be comparable if some excluded participants because of drusen suspicions while others could not screen their participants for smaller drusen using high resolution imaging. This is why the emergence of recent imaging methods allowing the precise visualization of small drusen is crucial. Studies such as retromode imaging[51] or gaze-dependent imaging[23] can both detect smaller drusen before a classic SD-OCT analysis. Even though it is currently impossible to know whether or not drusen will grow into larger and more severe forms, the important aspect today is to detect them at the earliest possible moment to track their progression and understand their development before critical and irreversible damage occurs. Healthstyle changes can also help slow down their growth and new drugs are currently being tested to further decelerate the formation of drusen. Our findings show that those small drusen could also be detected by looking at the changes in fixational eye movements during a fixation task.

Research on eye movements has existed for more than a century, and the recent infrared video eye trackers carried important promises with applications to the diagnostic, therapeutic and follow-up of neurologic and eye diseases. Pupil and corneal reflection-based eye-trackers remote tracking capabilities, accuracy and accessibility renewed the interest on eye movements to clinicians and psychologists. Research on FEM in particular revealed important insights on neurological diseases. However it is now demonstrated that such technology suffers from several limitations to study FEM. The reasons for this range from not covering the actual amplitude range of microsaccade, making researchers shift the amplitude-based definition of the microsaccades from limits of 0.2° to 1°[37,41,52,53], to basic recording of microsaccade dynamic (PSO: Artal, effect of pupil size on MS size, etc). Microsaccades amplitude measurement has been only recently found consistent with early recordings through the use of complex Adaptive Optics (AO) retinal imaging instruments. AO-SLO offered a welcomed capability in tracking the landing position of the stimulus onto the retina. The AO-FIO in the mode we used in this study does not reach as high image contrast as AO-SLO can.

However, it does not suffer from any distortion, unlike any SLO system whose scanning nature does not make it ideal for motion tracking. Using our retinal tracking method, we found an average healthy microsaccade amplitude of 6.3 arcminutes while patients with drusen had an average microsaccade amplitude of 13.8 arcminutes. In the past 20 years, FEM studies using pupil-based eye trackers have defined a microsaccade with amplitudes up to 1-2°, and basic fixation tasks often showed average amplitudes of 20-60 arcminutes. It is not impossible that the differences between controls and drusen participants in this study would not have been found using less precise but more available eye trackers, or a bigger fixation target since microsaccade amplitude is target-dependent[54] and we used a very small one.

In conclusion, a direct link between foveal drusen and fixation stability was found and fixational eye movements could be used as a biomarker to detect AMD at a pre-symptomatic stage. However, the improvement of precision and availability of eye-tracking methods is a key point to being able to use them as widespread biomarkers. In a more general way, in the past couple decades, it has become clear that FEM give unique signatures about a patient's neurological and physical health. Regular fixation tests could help control and track general health and redirect to different and more specific diagnostics depending on the results.

Acknowledgments

IHU FOReSIGHT (ANR-18-IAHU-01) ; SilverSight (ANR-18-CHIN-0002) ; OPTORETINA ERC (101001841) ; MACUSTAR (ask Michel)